ESKİŞEHİR TECHNICAL UNIVERSITY JOURNAL OF SCIENCE AND TECHNOLOGY
A- APPLIED SCIENCES AND ENGINEERING

2018, 19(3), pp. 768 - 783, DOI: 10.18038/aubtda.418710

DETERMINATION OF STRESS INTENSITY FACTORS IN AN ORTHOTROPIC STRIP WEAKENED BY TWO CRACKS

Elçin YUSUFOĞLU [1], İlkem TURHAN ÇETİNKAYA [2,*]

[1] Mathematics, Science and Art Faculty, Uşak University, Uşak, Turkey
[2] Mathematics, Science and Art Faculty, Dumlupınar University, Kütahya, Turkey

ABSTRACT

In this paper, stress intensity factors (SIFs) at the edges of the cracks in an elastic orthotropic strip weakened by two collinear cracks are determined. The problem consisted of two symmetrical cracks about the sides of the strip and axis *y*- is approached by Iterative method. Also, by reducing the problem to a system of Cauchy type singular integral equations, a Quadrature technique is used to calculate SIFs. Finally, extensive numerical results and detailed interpretations are given.

Keywords: Crack, Theory of elasticity, Quadrature approach, Iterative technique

1. INTRODUCTION

In fracture mechanics, determination of the SIFs in a cracked strip plays an important role, since it enables to estimate crack propagation. A great number of studies in this field have been done.

Shen and Fan [1] calculated mode I SIFs for a strip include two semi-infinite collinear cracks. Using complex function method, exact solutions are obtained. Also, Li and Fan [2] found the exact solutions for SIFs of two semi-infinite collinear cracks in a strip of one dimensional hexagonal quasicrystal by considering complex variable method.

Srivastava et.al. [3] considered an infinitely long elastic strip with two coplanar Griffith cracks. It is aimed to examine the interaction of shear waves. By using an integral transform method dynamic SIFs are obtained.

Zhou et.al., [4] studied a strip problem which involves two collinear symmetrical cracks. The problem is reduced to a set of triple integral equations with the help of Fourier transform and solved by Schmidts method.

Li [5] converted two cracks problem in an orthotropic strip into a singular integral equation by using the Fourier series method. A closed form solution is obtained for mode III SIFs.

Delale and Erdogan [6] determined the SIFs for the plane elastostatic problem in an infinite orthotropic strip and the obtained results are compared with isotropic results.

Dhaliwal and Singh [7, 8] examined the SIFs and crack energy in an isotropic elastic strip and layer weakened by two coplanar Griffith cracks, respectively. The obtained triple integral equations by Fourier transform are solved exactly.

*Corresponding Author: ilkem.turhan@dpu.edu.tr
Received: 26.04.2018 Accepted:05.09.2018

Erbas et.al., [9] considered a plane contact problem for an elastic orthotropic strip. They approached to the reduced singular integral equation by iterative solution method for thick strip and by a direct asymptotic procedure for a thin strip.

The detailed studies for singular integral equations are done by Erdogan et.al., [10]. Numerical methods for the solution of singular integral equations with Cauchy kernel are described. Some examples of the crack problems are solved to show the application of the methods.

Yusufoğlu and Turhan [11, 12] considered an orthotropic strip problem including a crack. The problem is reduced to a singular integral equation. The reduced singular integral equation is solved to determine normalized SIFs by Iterative method and Gauss Chebyshev quadrature rule, respectively. It has seen that, the results are convenient with the results in [13].

This study consists of five sections. In the second section, an orthotropic strip weakened by two symmetric cracks is considered. The problem is solved by Iterative method. Analytical expressions of mode I SIFs are obtained. In the third section, the same problem is approached by Gauss quadrature formulas. In the fourth section, considering three different orthotropic materials, numerical results are given. Finally, in the conclusion section, the results are interpreted and the effect of loading conditions and the distance between cracks on the SIFs are analyzed.

2. SOLUTION OF MIXED BOUNDARY VALUE PROBLEM CORRESPONDING TO TWO CRACKS LOCATED SYMMETRICALLY ABOUT AXIS y- BY ITERATIVE METHOD

In this section, a strip problem weakened by two symmetrical cracks is considered. The problem is approached by Iterative method to obtain SIFs. Also, the similar strip problem weakened by a crack has been solved by Iterative method in [11]. The SIF values at the edges of the cracks are obtained and the results have been compared with the results in [13]. The compatibility of these results has been seen.

In this problem, it is assumed that, there are two collinear cracks in an elastic orthotropic strip located on $x \in [-b,-a] \cup [a,b]$ and the crack sides are loaded by uniformly distributed pressure of magnitude $q(x)$.

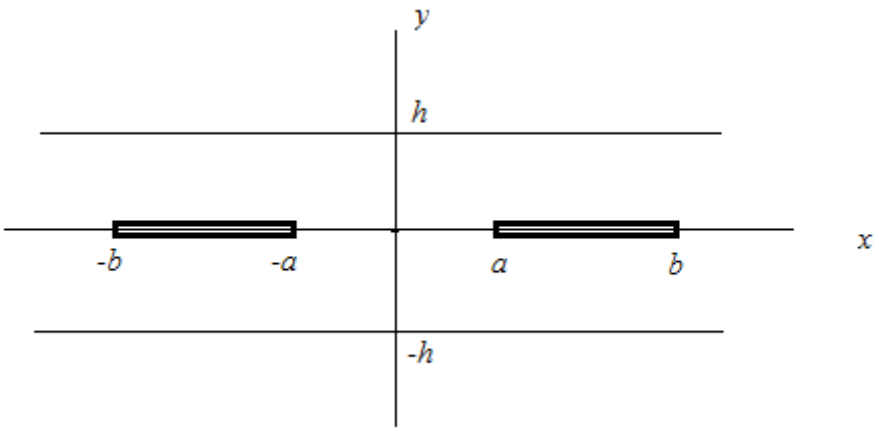

Figure 1. Geometry of the problem

The boundary conditions of the related elasticity problem are as follows:

$$\upsilon(x,\pm h)=\sigma_{xy}(x,\pm h)=0,\ \sigma_{xy}(x,0)=0,\ |x|<\infty,\ \upsilon(x,0)=0,\ x\in R\setminus[-b,-a]\cup[a,b],$$
$$\sigma_y(x,0)=-q(x),\ x\in[-b,-a]\cup[a,b]. \tag{1}$$

Here, υ denotes the vertical displacement; σ_{xy} and σ_y are shear and normal stress components, respectively.

Considering the symmetry of the related problem about the $x-$coordinate, the auxiliary problem for a strip of thickness h with the boundary conditions is given as

$$\upsilon(x,h)=\sigma_{xy}(x,h)=0,\quad \sigma_{xy}(x,0)=0,\quad \upsilon(x,0)=\hat{\gamma}(x),\quad |x|<\infty,$$
$$\hat{\gamma}(x)=\begin{cases}\gamma(x), & x\in[-b,-a]\cup[a,b]\\ 0, & \textit{otherwise.}\end{cases} \tag{2}$$

Here, the function $\gamma(x)$ denotes the displacements of points on the crack sides. By considering the continuity of the function $\hat{\gamma}(x)=\upsilon(x,0)$, the following additional condition can be obtained:

$$\gamma(\pm a)=\gamma(\pm b)=0. \tag{3}$$

Similar to the given procedure in [11,18,19], considering basic equations of elasticity theory, Fourier technique and Eqs. (1)-(3), the following integral equation is obtained

$$\int_a^b \gamma'(\xi)\left[M\left(\frac{\xi+x}{h}\right)+M\left(\frac{\xi-x}{h}\right)\right]d\xi=-\frac{\pi h q(x)}{\Delta} \tag{4}$$
$$M(t)=\int_0^\infty \frac{1}{L(u)}\sin(ut)du,\quad x\in[a,b],$$

where,

$$L(u)=\frac{\kappa_2-\kappa_1}{\kappa_2\coth(\kappa_1 u)-\kappa_1\coth(\kappa_2 u)},\quad \Delta=\frac{E_2\kappa_1\kappa_2}{(1-\nu_{32}\nu_{23})(\kappa_1+\kappa_2)}.$$

Lemma 1: *For all values of* $|t|<\infty$ *the kernel* $M(t)$

$$M(t)=\frac{1}{t}+F(t),\quad F(t)=\int_0^\infty\left(\frac{1}{L(u)}-1\right)\sin(ut)du \tag{5}$$

is true, also $F(t)$ *is a regular function in the domain of* $\{(t,\tau)\ |t|<\infty,|\tau|<2\}$ *as a function of the complex variable* $w=t+i\tau$. *When* $|t|<2$, *the function of* $F(t)$ *can be presented with absolute convergence series as*

$$F(t)=\sum_{n=0}^{\infty} d_n t^{2n+1},$$

where,

$$d_n = \frac{(-1)^{n+1}}{(2n+1)!}\int_0^{\infty}\left[1-\frac{1}{L(u)}\right]u^{2n+1}du\ ,\ n=0,1,2,...\ [14,\text{ p.29}].$$

By inserting Eq. (5) into Eq. (4) and converting the integral equation into dimensionless form,

$$\int_{-1}^{1}\frac{\tilde{w}(u)}{u-x_1}du = -\pi p(t) - \frac{b^2-a^2}{2h}\int_{-1}^{1}\tilde{w}(u)\tilde{K}(u,t)du \tag{6}$$

is obtained. Here,

$$\tilde{w}(u) = w\left(\frac{b^2-a^2}{2}u+\frac{b^2+a^2}{2}\right)\ ,\quad w(\tau)=\gamma'\left(\sqrt{\tau}\right)\ , \tag{7}$$

$$\tilde{K}(u,t) = K\left(\frac{b^2-a^2}{2}u+\frac{b^2+a^2}{2},t\right),\quad K(\tau,t)=\frac{1}{2\sqrt{\tau}}\left[F\left(\frac{\sqrt{\tau}+\sqrt{t}}{h}\right)+F\left(\frac{\sqrt{\tau}-\sqrt{t}}{h}\right)\right],$$

$$p(t)=\frac{q\left(\sqrt{t}\right)}{\Delta}\ ,\qquad x_1=-\frac{b^2+a^2-2t}{b^2-a^2}\ ,\qquad t=x^2\ .$$

The Cauchy-type singular integral equation (6) may be regularized. By considering the method of Carlemann and Vekua, the following lemma can be written [17]:

Lemma 2. *Every solution of Eq.(6) in the class of* $L_\beta(-1,1),\ \ 1<\beta<\frac{4}{3}$ *is also the solution of the following integral equation:*

$$\tilde{w}(x_1)=\frac{1}{\sqrt{1-x_1^{\,2}}}\left[\overline{\Psi_0}(x_1)+\frac{b^2-a^2}{\pi^2 2h}\int_{-1}^{1}\frac{\sqrt{1-u^2}}{u-x_1}du\int_{-1}^{1}\tilde{w}(\eta)\tilde{K}(\eta,u)d\eta\right], \tag{8}$$

$$\overline{\Psi_0}(x_1)=\frac{N}{\pi}+\frac{1}{\pi}\int_{-1}^{1}\frac{p(u)\sqrt{1-u^2}}{u-x_1}du\ . \tag{9}$$

The inverse of this lemma is true if $p(x)\in L_\alpha(-1,1),\ \ \alpha>4$ [15]. Here, $L_\alpha(a,b)$ is the space of Lebesgue integrable functions of order *α* in the interval *(a,b).*

Theorem 1. *If* $p(x)\in H_n^{\alpha}(-1,1),\ \ \alpha>0,\ \ n\geq 0$ *and Eq. (8) has solution in the class of* $L_\beta(-1,1),\ \ 1<\beta<\frac{4}{3}$*, then the solution can be presented for* $\forall\lambda\in(0,\infty)$ *as follows,*

$$\tilde{w}(x_1)=\frac{\Psi(x_1)}{\sqrt{1-x_1^{\,2}}}\ , \tag{10}$$

where $\Psi(x_1)\in C_n(-1,1)$*;* $H_n{}^{\alpha}(-1,1)=\left\{f\,\middle|\,f\in C_n(-1,1),\quad f^{(n)}\in H^{\alpha}[-1,1]\right\}$ [14]. Here, $C_n(-1,1)$ and $H^{\alpha}[-1,1]$ are the spaces of continuous differentiable functions of order *n* and the spaces of functions that satisfy Holder condition in the interval *(-1,1)*, respectively.

Now, by using Eq. (10) we can rewrite the following equations instead of Eq. (9);

$$\Psi(x_1) = \overline{\Psi_0}(x_1) + A\Psi\,,\ A\Psi = \int_{-1}^{1} \Psi(u)\frac{G(u,x_1)}{\sqrt{1-u^2}}du\ , \tag{11}$$

where,

$$G(u,x_1) = \frac{b^2-a^2}{2\pi^2 h}\int_{-1}^{1}\frac{\sqrt{1-\eta^2}}{\eta - x_1}\tilde{K}(u,\eta)d\eta. \tag{12}$$

Lemma 3. *Let $p(x_1) \in H^{\alpha}(-1,1)$, $\alpha > 0$. The function $\overline{\Psi_0}(x_1)$ defined by Eq. (9) is a continuous function.*

Rewritting Eq. (11) as $\Psi = B\Psi$, where, $B\Psi = \Psi_0 + A\Psi$,

the following theorem can be given similarly Banach theorem.

Theorem 2. *Let the conditions of Lemma 3 are satisfied. Then, for every λ, $\lambda > \lambda_\infty = \frac{1}{2}\left(D_0 + \sqrt{D_0^{\,2} + 2D_1}\right)$, $D_0 = \max|F(t)|$, $D_1 = \max|F'(t)|$, $t \in [0,\ \infty)$, operator B has an only and only fixed point in the class of continious functions. The fixed point is the limit of the sequence of iterations of Ψ.*

To use Eqs. (11) and (12) in the sequence of iterations of Ψ leads to following formula for the general term of sequence $\Psi_n(x_1)$:

$$\Psi_n(x_1) = \frac{N}{\pi}\left[1 + \int_{-1}^{1}\frac{\sum_{k=1}^{n} G_k(u,x_1)}{\sqrt{1-u^2}}du\right] + \frac{1}{\pi}\int_{-1}^{1} p(s)\sqrt{1-s^2}\left[\frac{1}{s-x_1} + \int_{-1}^{1}\frac{\sum_{k=1}^{n} G_k(u,x_1)}{(s-u)\sqrt{1-u^2}}du\right]ds, \tag{13}$$

where,

$$G_1(u,x_1) = G(u,x_1),\ G_k(u,x_1) = \int_{-1}^{1}\frac{G_1(u,\tau_1)G_{k-1}(\tau_1,x_1)}{\sqrt{1-\tau_1^{\,2}}}d\tau_1,\quad k = 2,3,...,n\ . \tag{14}$$

Considering Eq. (13) and using the iterated kernels (14) together with Eqs. (10) and (12), the solution for integral equation (8) can be obtained as

$$\tilde{w}(x_1)=\frac{1}{\pi\sqrt{1-x_1^2}}\int_{-1}^{1}p(s)\sqrt{1-s^2}\left\{\frac{1}{s-x_1}+\frac{\left(1-\varepsilon^2\right)^2 d_1 x_1}{4\lambda^4}+\frac{d_2}{16\lambda^6}\left(12x_1\varepsilon^2+\varepsilon^6 x_1 s\right.\right.$$
$$-12x_1\varepsilon^6+10x_1^2\varepsilon^6+3x_1 s\varepsilon^2-3x_1 s\varepsilon^4+12x_1\varepsilon^4+30x_1^2\varepsilon^2-30x_1^2\varepsilon^4-5\varepsilon^6-15\varepsilon^2$$
$$\left.\left.+15\varepsilon^4-x_1 s-12x_1-10x_1^2+5\right)+O\left(\lambda^{-8}\right)\right\}ds+\frac{N}{\pi\sqrt{1-x_1^2}}\left\{1+\frac{1}{2\lambda^2}d_0 x_1\left(-1+\varepsilon^2\right)\right.$$
$$-\frac{d_1}{8\lambda^4}\left(6x_1^2-8x_1\varepsilon^4+6x_1^2\varepsilon^4-12x_1^2\varepsilon^2+6\varepsilon^2-3+8x_1-3\varepsilon^4\right)+\frac{1}{16\lambda^6}\left[d_0 d_1\left(3\varepsilon^4 x_1\right.\right. \qquad (15)$$
$$\left.-\varepsilon^6 x_1-3\varepsilon^2 x_1+x_1\right)+d_2\left(44x_1\varepsilon^4+20+30x_1^3\varepsilon^2-40x_1^2\varepsilon^6+40x_1^2\varepsilon^2-44x_1\varepsilon^2\right.$$
$$-30x_1^3\varepsilon^4+40x_1^2\varepsilon^4-20\varepsilon^4+28x_1\varepsilon^6+10\varepsilon^6 x_1^3-10x_1^3-20\varepsilon^2-28x_1-40x_1^2$$
$$\left.\left.\left.+20\varepsilon^6\right)+O\left(\lambda^{-8}\right)\right]\right\}.$$

Here, it is assumed that, $\varepsilon=\frac{a}{b}$, $\frac{1}{\lambda}=\frac{b}{h}$.

Now, we will obtain analytical expressions of the SIFs $K_I(a)$ and $K_I(b)$. Mode I SIFs occurred in a crack located on *[a,b]* are defined as,

$$K_I(a)=\lim_{x\to a+0}\sqrt{2\pi(x-a)}\,\Delta\gamma'(x),\quad K_I(b)=-\lim_{x\to b-0}\sqrt{2\pi(b-x)}\,\Delta\gamma'(x). \qquad (16)$$

During the analysis, we will consider two different loading condition given in Figure 2.

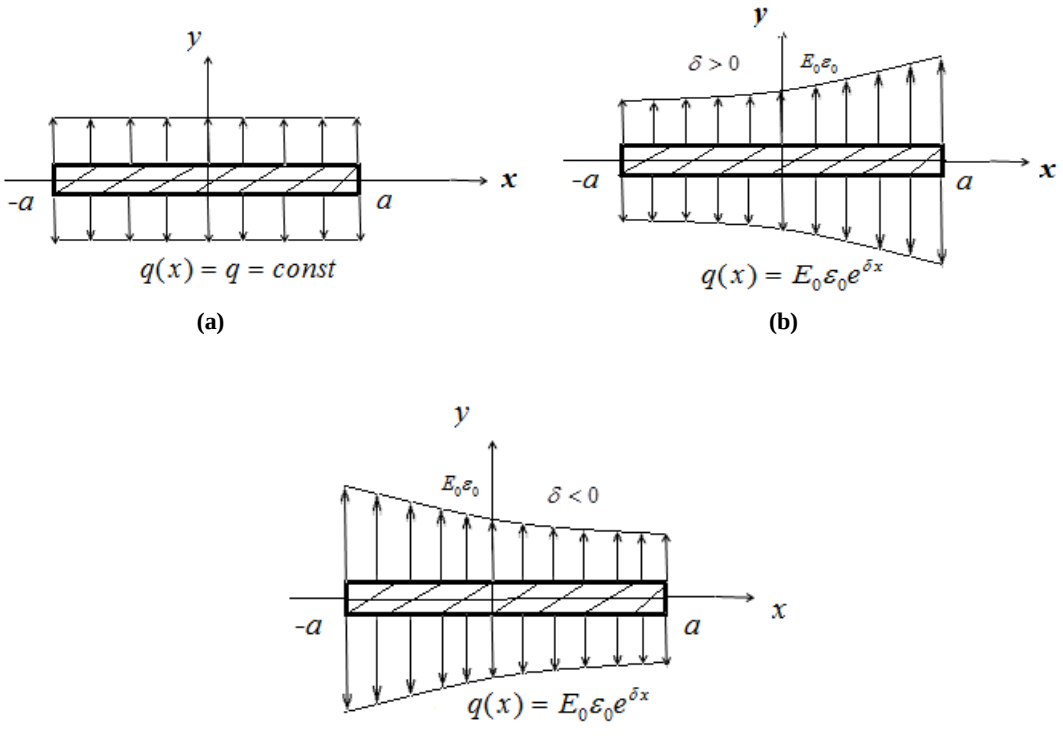

Figure 2. Geometry of loading conditions: (a) Uniform crack surface pressure; (b) Fixed grip loading; (c) Fixed grip loading.

By considering the first loading condition, i.e., $p(s)=q/\Delta$, in Eq. (15) and using Eqs. (7), the derivative of the function describing vertical displacements of the points on the crack sides is obtained:

$$\gamma'(x)=\frac{1}{A(x)}\left\{\frac{Nb^2\left(1-\varepsilon^2\right)}{2\pi}+\frac{q\left(b^2+\varepsilon^2b^2-2x^2\right)}{2\Delta}+\frac{Nd_0}{4\pi\lambda^2}\left(b^2+\varepsilon^2b^2-2x^2\right)\left(1-\varepsilon^2\right)\right.$$
$$+\frac{d_1}{16b^4\Delta\pi\lambda^4}\left[q\pi\left(b^6-b^6\varepsilon^2-2b^4x^2-b^6\varepsilon^4+4b^4\varepsilon^2x^2+b^6\varepsilon^6-2b^4\varepsilon^4x^2\right)\right. \quad (17)$$
$$\left.\left.+N\Delta\left(1-\varepsilon^2\right)\left(8x^2b^4+8x^2\varepsilon^2b^4-24x^4b^2+5\varepsilon^4b^6-2\varepsilon^2b^6+5b^6\right)\right]\right\}+O\left(\lambda^{-6}\right),$$

where

$$A(x)=\sqrt{-b^4\varepsilon^2+b^2x^2+b^2\varepsilon^2x^2+x^4}\ .$$

Applying Eq. (17) in the formulas (16), SIFs at the edges *a* and *b* are obtained as follows, respectively

$$K_I(a)=\frac{\sqrt{a}\sqrt{1-\varepsilon^2}\left(N\Delta+\pi q\right)}{2\varepsilon\sqrt{\pi}}+\frac{d_0\sqrt{a}N\Delta\left(1-\varepsilon^2\right)^2}{4\varepsilon\sqrt{\pi}\sqrt{1-\varepsilon^2}\lambda^2}-\frac{d_1\sqrt{a}\sqrt{1-\varepsilon^2}}{16\lambda^4\varepsilon\sqrt{\pi}}\left[N\Delta\left(11\varepsilon^4-6\varepsilon^2-5\right)\right.$$
$$\left.+q\pi\left(-\varepsilon^4+2\varepsilon^2-1\right)\right],$$
$$K_I(b)=\frac{\sqrt{b}\sqrt{1-\varepsilon^2}\left(N\Delta+\pi q\right)}{2\sqrt{\pi}}+\frac{d_0\sqrt{b}N\Delta\left(1-\varepsilon^2\right)\sqrt{1-\varepsilon^2}}{4\sqrt{\pi}\sqrt{\varepsilon}\lambda^2}-\frac{d_1\sqrt{b}\sqrt{1-\varepsilon^2}}{16\lambda^4\sqrt{\pi}}\left[N\Delta\left(5\varepsilon^4+6\varepsilon^2-11\right)\right.$$
$$\left.+q\pi\left(-\varepsilon^4+2\varepsilon^2-1\right)\right].$$

3. SOLUTION OF MIXED BOUNDARY VALUE PROBLEM CORRESPONDING TO TWO CRACKS LOCATED SYMMETRICALLY ABOUT AXIS y- BY GAUSS QUADRATURE FORMULAS

In this section, two symmetrical cracks problem given in Figure 1 is solved with the help of Gauss quadrature formulas. Similar problem corresponding to a crack is considered in [12]. The problem has been approached by Gauss-Chebyshev quadrature. The obtained values of SIFs have been compared with results in [11,13] and it is concluded that the present results agree well with those of references.

For two cracks problem, the following system of singular integral equation is obtained:

$$\sum_{j=1}^{2}\int_w\frac{\gamma_j'(\xi)}{\xi-x}d\xi+\frac{1}{h}\sum_{j=1}^{2}\int_w\gamma_j'(\xi)F\left(\frac{\xi-x}{h}\right)d\xi=-\frac{\pi}{\Delta}q(x), \quad (18)$$

where, $q(x)=\begin{cases}q_1(x), & x\in(-b,-a)\\ q_2(x), & x\in(a,b)\end{cases}$.

Similarly to Eq. (3), with the help of the following continuity condition,

$$\gamma_i(\pm a)=\gamma_i(\pm b)=0,\ \ i=1,2,$$

the following integral equations are obtained:

$$\int_{-b}^{-a} \gamma_1'(\xi)\,d\xi = 0, \qquad \int_{a}^{b} \gamma_2'(\xi)\,d\xi = 0. \tag{19}$$

Substituting the variables

$$x = s_i + r_i t\,,\ \xi = s_j + r_j \tau\,,\ s_i = \frac{\pm(b+a)}{2}\,,\ r_i = \frac{b-a}{2}$$

in Eqs. (18) and (19), the system of singular integral equations turn into dimensionless forms are obtained as

$$\int_{-1}^{1} \frac{\varphi_i(\tau)}{\tau - t}\,d\tau + \sum_{\substack{j=1 \\ i\neq j}}^{2} \int_{-1}^{1} \frac{\varphi_j(\tau)}{\tau - \dfrac{r_i}{r_j}t + \dfrac{s_j - s_i}{r_j}}\,d\tau + \sum_{j=1}^{2} \int_{-1}^{1} \varphi_j(\tau) F_{ij}^{*}(\tau, t)\,d\tau = f_i(t), \tag{20}$$

$$\int_{-1}^{1} \varphi_i(\tau)\,d\tau = 0\,, \tag{21}$$

where,

$$\varphi_j(\tau) = \gamma_j'\left(s_j + r_j\tau\right),\ F_{ij}^{*}(\tau, t) = \frac{r_j}{h} F_{ij}\left(\frac{r_j\tau - r_i t + s_j - s_i}{h}\right),\ f_i(t) = -\frac{\pi q_i\left(s_i + r_i t\right)}{\Delta}\,,\quad i = 1,2$$

In this section, the solution of reduced system of singular integral equations (20),(21) is approached by the procedure given in [16]. So, according to Muskheleshvili [17], the solution can be obtained as

$$\varphi_j(t) = \frac{\phi_j(t)}{\sqrt{1-t^2}}\,,\ j = 1,2\,. \tag{22}$$

Substituting Eqs. (22) into Eqs. (20)-(21) and defining the function $\phi_j(t)$ by Lagrange interpolation polynomials as

$$\phi_n^{(j)} = \sum_{m=1}^{n} \frac{\phi_j(\tau_m) T_n(t)}{(t - \tau_m) T_n'(\tau_m)}\,,$$

the following system of singular integral equation is obtained:

$$\int_{-1}^{1} \frac{\phi_n^{(i)}(\tau)}{(\tau - t)\sqrt{1-\tau^2}}\,d\tau + \sum_{\substack{j=1 \\ i\neq j}}^{2} \int_{-1}^{1} \frac{\phi_n^{(j)}(\tau)}{\left(\tau - \dfrac{r_i}{r_j}t + \dfrac{s_j - s_i}{r_j}\right)\sqrt{1-\tau^2}}\,d\tau + \sum_{j=1}^{2} \int_{-1}^{1} \frac{\phi_n^{(j)}(\tau) F_{ij}^{*}(\tau, t)}{\sqrt{1-\tau^2}}\,d\tau = f_i(t), \tag{23}$$

$$\int_{-1}^{1} \frac{\phi_n^{(i)}(\tau)}{\sqrt{1-\tau^2}}\,d\tau = 0\,,\ i = 1,2\,. \tag{24}$$

Here, $T_n(t)$ denotes the Chebyshev polynomials of the first kind, τ_m, ($m = 1,2,...,n$) are the roots of the Chebyshev polynomials of the first kind and

$$\phi_n^{(j)}(\tau_m) = \phi_j(\tau_m)$$

is valid.

By considering the following known formulas for Chebyshev polynomials of first and second kind [20]

$$\int_{-1}^{1} \frac{T_n(\tau)}{(\tau - t)\sqrt{1-\tau^2}} d\tau = \pi U_{n-1}(t), \qquad \frac{U_{n-1}(\tau_m)}{T_n'(\tau_m)} = \frac{1}{n}$$

and using appropriate Gauss-Chebyshev integration formula for Eq. (22), next, setting $t = t_m$ ($m=1,2,\ldots,n-1$) in equation (23), where t_m are roots of the polynomial $U_{n-1}(t)$, the system of linear equations is obtained:

$$\sum_{j=1}^{2}\sum_{m=1}^{n}\left[\frac{1}{\tau_m - (r_i / r_j)t_k + (s_j - s_i)/r_j} + F_{ij}^{*}(\tau_m, t_k)\right]\frac{\pi\phi_j(\tau_m)}{n} = f_i(t_k).$$

The additioal condition can be obtained by using the same procedure as follows,

$$\sum_{m=1}^{n}\frac{\pi}{n}\phi_j(\tau_m) = 0.$$

4. NUMERICAL RESULTS

In this section, we will analyse the effect of the orthotropy and relative thickness on the normalized SIFs. In accordance with this purpose, three kinds of orthotropic materials given in Table 1 are considered. Here, the coefficients are the elements of the compliance matrix which is the inverse of stiffness matrix obtained by Hooke's law for an orthotropic material in case of plane strain. Table 1 is rewritten as transformation of stiffness parameters in [21].

Table 1. Compliance parameters for selected materials

Material i	s_{11}	s_{12}	s_{22}	s_{66}
1	$0.101\text{x}10^{-9}$	$-0.209\text{x}10^{-10}$	$0.676\text{x}10^{-10}$	$0.141\text{x}10^{-9}$
2	$0.977\text{x}10^{-10}$	$-0.757\text{x}10^{-11}$	$0.244\text{x}10^{-10}$	$0.141\text{x}10^{-9}$
3	$0.244\text{x}10^{-10}$	$-0.757\text{x}10^{-11}$	$0.977\text{x}10^{-10}$	$0.141\text{x}10^{-9}$

Here and in the other tables, Material i denotes the names of three materials with different orthotropic properties. From Table 1, it is obvious that Materials 2 and 3 are same except a 90 degree rotation of orthotropy. Since compliance matrix of a material is the inverse of the stiffness matrix, from Table 1, it can be seen that while Material 3 has the highest orthotropy, Material 2 has weakest orthotropy in crack line direction.

During the analyses, two different loading conditions i.e., uniform crack surface pressure and fixed-grip loading are considered to examine the effect of the degree of orthotropy and relative thickness on the SIFs. The loads are defined as $q(x) = q = const$ and $q(x) = E_0\varepsilon_0 e^{\delta x}$ in the cases of the uniform crack surface pressure and the fixed-grip loading, respectively. For the fixed-grip loading, the notations $\varepsilon_x(\infty, y) = \varepsilon_0$, $E_0 = c_{11} - c_{12}^2 / c_{22}$ are used.

The SIF values are calculated for the strips made from these materials under these two different loading conditions by using Gauss quadrature method and Iterative method. Also, in references [11-13], the strip problems weakened by a crack are also solved by Iterative method, Gauss-Chebyshev quadrature and Series method, respectively. The presented tables and graphics underline the compatibilty of the results for SIFs.

Figures 3-10 present the normalized SIFs for three kinds of material and under uniform crack surface pressure. Figures 3-5 give the effect of the relative thickness on right and left edge of SIFs, for considered three materials. It is established that, the crack propagation starts at $x=\pm a$. Also, while the relative thickness of the strip increases, SIFs increase too. It is obvious that while ε increases, the distance between the cracks increases, too. From Figures 6-8, when ε increases the SIFs at the edge a decrease and critical load increases. Figures. 9-10 show the effect of the relative thickness on the normalized SIFs at the edges a and b, for all materials and $\varepsilon = 0.5$, respectively. Since Material 3 has the highest orthotrophy, the SIFs in the strip made from Material 3 would be biggest at the both edges.

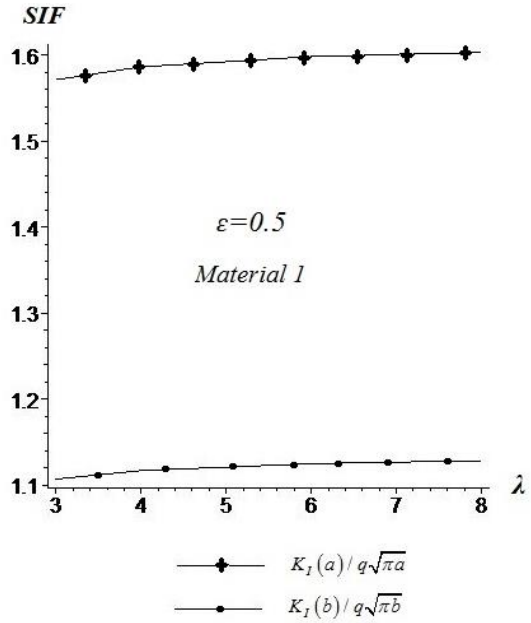

Figure 3. The effect of relative thickness on SIFs for Material 1 and $\varepsilon = 0.5$.

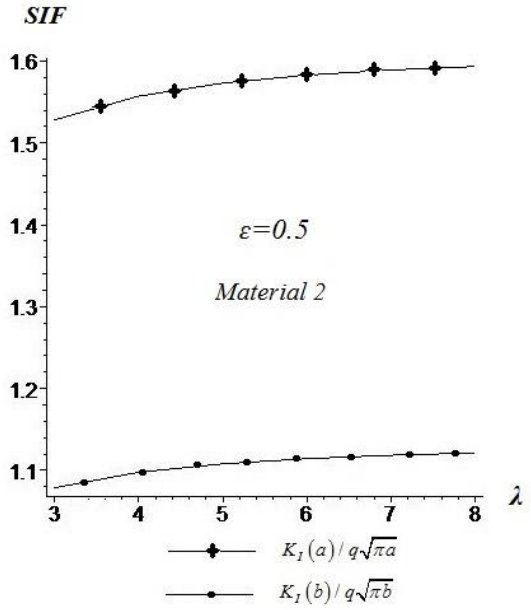

Figure 4. The effect of relative thickness on SIFs for Material 2 and $\varepsilon = 0.5$.

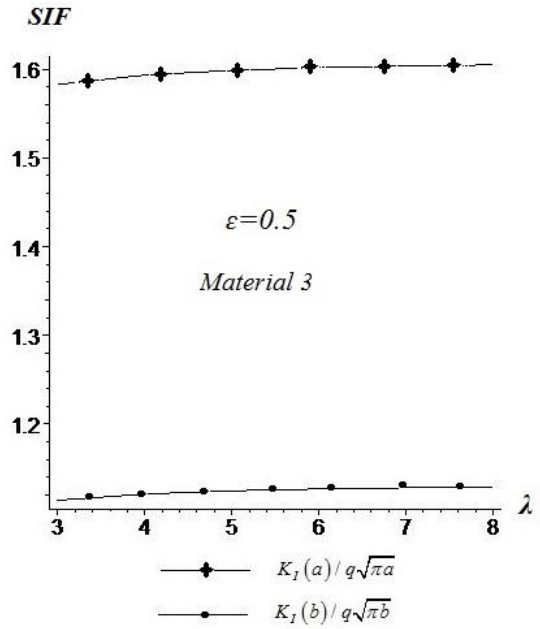

Figure 5. The effect of relative thickness on SIFs for Material 3 and $\varepsilon = 0.5$.

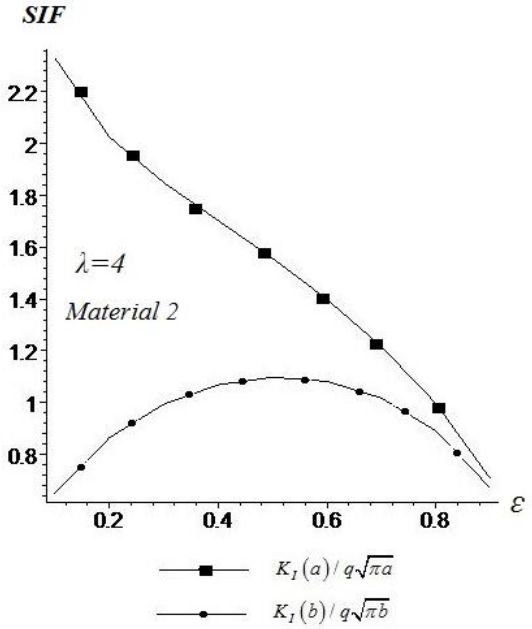

Figure 7. The effect of distance between cracks on SIFs for Material 2 and *λ=4.*

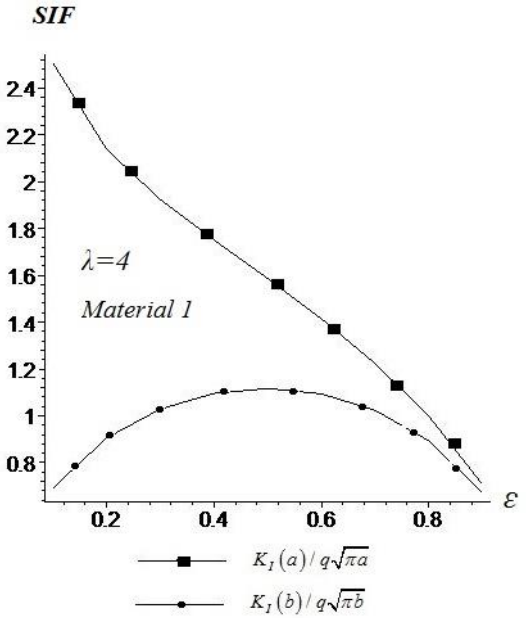

Figure 6. The effect of distance between cracks on SIFs for Material 1 and *λ=4.*

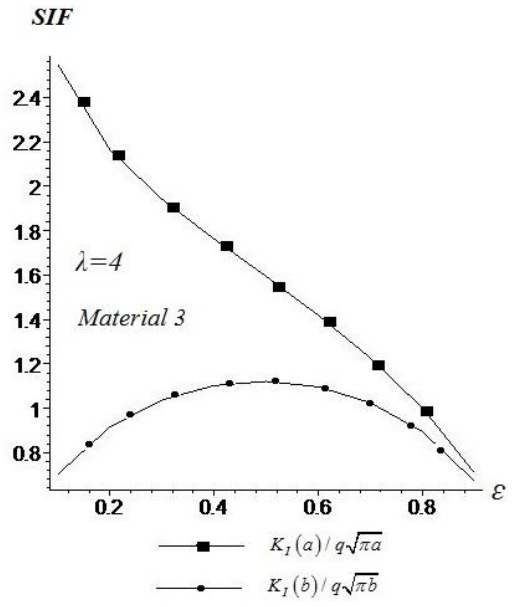

Figure 8. The effect of distance between cracks on SIFs for Material 3 and *λ=4.*

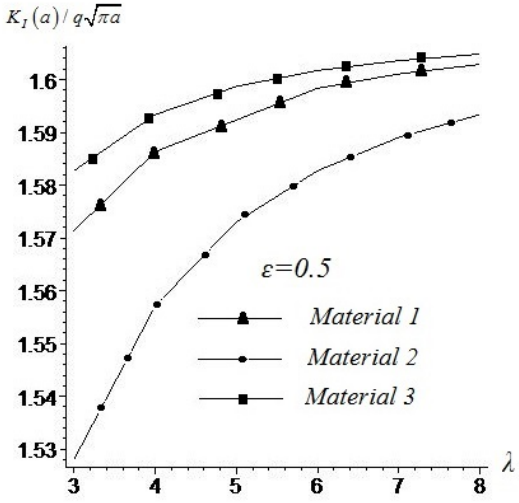

Figure 9. The effect of the relative thickness on the normalized SIFs at the edge a of the crack for all materials and $\varepsilon = 0.5$.

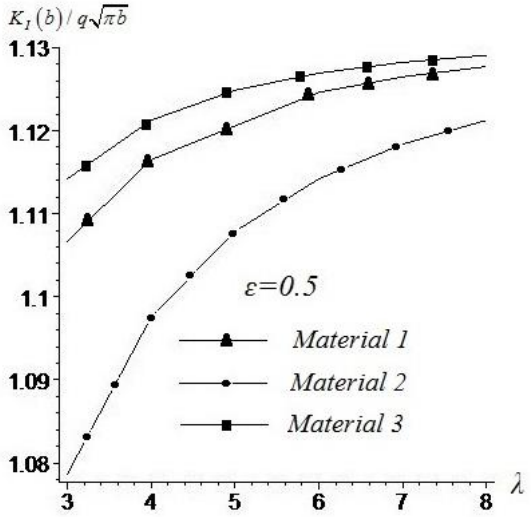

Figure 10. The effect of the relative thickness on the normalized SIFs at the edge b of the crack for all materials and $\varepsilon = 0.5$.

Table 2 presents the normalized SIFs correspond to the value of the material orthotropy parameter E_1/E_2 under uniform crack surface pressure. $E_1/E_2=1$ correspond to the isotropic material. As is seen from Table 2, while the anisotropy properties of the material from which the strip is made increase SIFs increase and the resistance of the strip decreases. In Table 2, the results are compared by Gauss Quadrature method and Iterative method to verify the validity of the results.

Table 2. The normalized SIFs correspond to the value of the material orthotropy parameter E_1/E_2 under uniform crack surface pressure.

		$\lambda=4$				$\lambda=6$			
		$K_I(-a)/q\sqrt{\pi a} = K_I(a)/q\sqrt{\pi a}$		$K_I(-b)/q\sqrt{\pi b} = K_I(b)/q\sqrt{\pi b}$		$K_I(-a)/q\sqrt{\pi a} = K_I(a)/q\sqrt{\pi a}$		$K_I(-b)/q\sqrt{\pi b} = K_I(b)/q\sqrt{\pi b}$	
E_1/E_2	ε	*Gauss Quadrature Method*	*Iterative Method*	*Gauss Quadrature Method*	*Iterative Method*	*Gauss Quadrature Method*	*Iterative Method*	*Gauss Quadrature Method*	*Iterative Method*
1	0.3	1.9132	1.9147	1.0238	1.0253	1.9485	1.9489	1.0413	1.0415
	0.5	1.5822	1.5830	1.1138	1.1149	1.5962	1.5963	1.1231	1.1232
	0.7	1.2229	1.2233	1.0226	1.0230	1.2266	1.2266	1.0255	1.0256
5	0.3	1.9537	1.9541	1.0440	1.0441	1.9682	1.9685	1.0515	1.0516
	0.5	1.5983	1.5983	1.1246	1.1246	1.6041	1.6041	1.1285	1.1285
	0.7	1.2271	1.2271	1.0260	1.0260	1.2287	1.2287	1.0273	1.0273
10	0.3	1.9643	1.9646	1.0495	1.0496	1.9731	1.9734	1.0541	1.0542
	0.5	1.6025	1.6025	1.1274	1.1275	1.6060	1.6060	1.1299	1.1299
	0.7	1.2283	1.2283	1.0269	1.0269	1.2292	1.2292	1.0277	1.0277
25	0.3	1.9741	1.9744	1.0546	1.0547	1.9775	1.9778	1.0564	1.0565
	0.5	1.6064	1.6064	1.6064	1.1302	1.6078	1.6078	1.1311	1.1312
	0.7	1.2293	1.2293	1.0278	1.0278	1.2297	1.2297	1.0281	1.0281

Figures 11-15 show the normalized SIFs for these three materials under fixed-grip loading. Figures 11-13 give the effect of the distance between cracks on SIFs for all tip materials. So, when cracks's length increases, the SIFs increase too. Figures 14-15 give the effect of relative thickness on SIFs under fixed-grip loading for all tips materials given in Table 1. When relative thickness of the strip increases, SIFs increase independently of strip material. Since Material 3 has the highest orthotropy in crack line direction, the normalized SIFs are the highest at the crack edges in the strip composed of Material 3. Likewise, since, Material 2 has weakest orthotropy in crack line direction, the normalized SIFs are the lowest at the crack edges in the strip composed of Material 2. Figure 16 shows the SIFs corresponding to material orthotrophy parameter values E_1/E_2 under fixed-grip loading for a strip

weakened by two cracks. It can be interpreted, when the material orthotrophy parameter values E_1/E_2 increase, SIFs also increase and then strip resistance decreases.

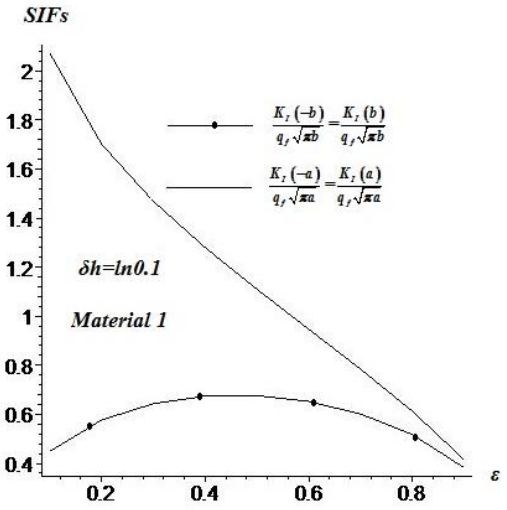

Figure 11. The effect of distance between cracks on SIFs for Material 1 under fixed grip loading given by $q_1(x)=q_f e^{-\delta x}$, $q_2(x)=q_f e^{\delta x}$.

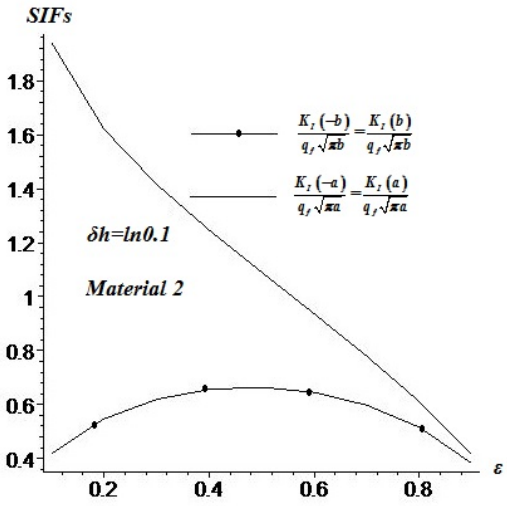

Figure 12. The effect of distance between cracks on SIFs for Material 2 under fixed grip loading given by $q_1(x)=q_f e^{-\delta x}$, $q_2(x)=q_f e^{\delta x}$.

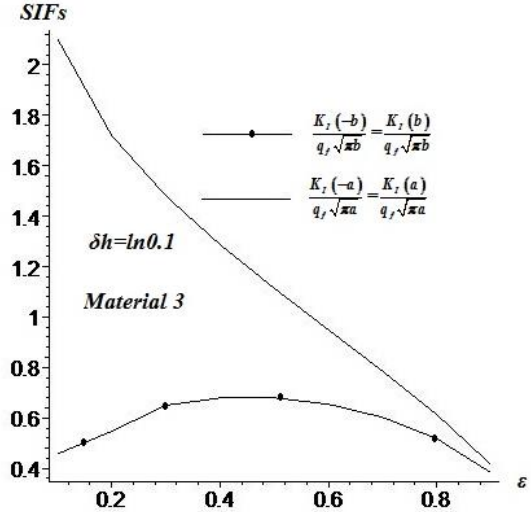

Figure 13. The effect of distance between cracks on SIFs for Material 3 under fixed grip loading given by $q_1(x)=q_f e^{-\delta x}$, $q_2(x)=q_f e^{\delta x}$.

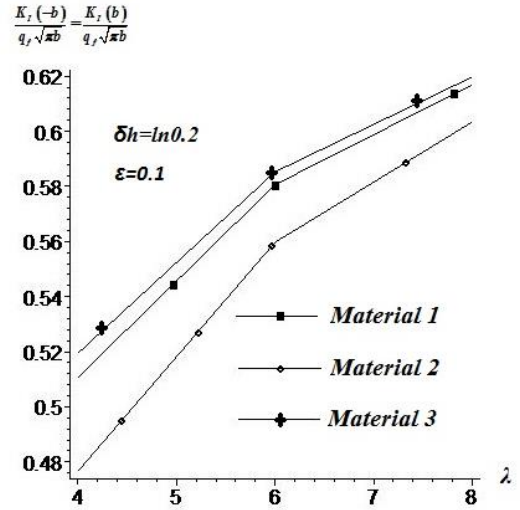

Figure 14. The effect of relative thickness on SIFs at the edges *b* under fixed grip loading given by $q_1(x)=q_f e^{-\delta x}$, $q_2(x)=q_f e^{\delta x}$.

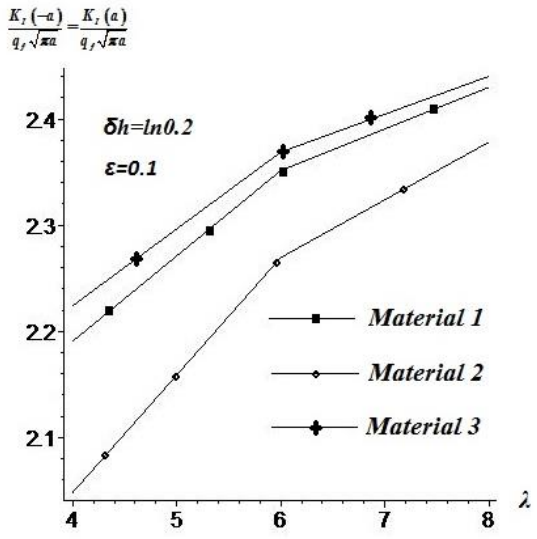

Figure 15. The effect of relative thickness on SIFs at the edges *a* under fixed grip loading given by $q_1(x)=q_f e^{-\delta x}$, $q_2(x)=q_f e^{\delta x}$.

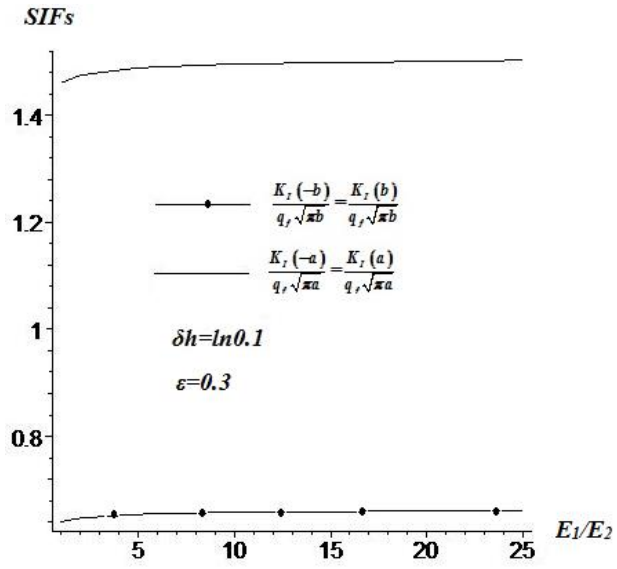

Figure 16. The normalized SIFs correspond to the value of the material orthotropy parameter E_1/E_2 under fixed grip loading given by $q_1(x)=q_f e^{-\delta x}$, $q_2(x)=q_f e^{\delta x}$, for $\lambda=4$.

5. CONCLUSION

In this study, the problem is approached by Gauss Quadrature formulas and Iterative method. It is established that, when the distance between the cracks increases, i.e., $\varepsilon=a/b$ increases, normalized SIFs decrease. Also, it is obvious that the crack propagation starts at $x=\pm a$. When the crack sides are loaded by uniform crack surface pressure it has seen that $K_I(-a)/\left(q\sqrt{\pi a}\right)=K_I(a)/\left(q\sqrt{\pi a}\right)$ and $K_I(-b)/\left(q\sqrt{\pi b}\right)=K_I(b)/\left(q\sqrt{\pi b}\right)$. When the crack sides are loaded by fixed-grip loading, if loading conditions are given symmetrically as $q_1(x)=q_f e^{-\delta x}$, $q_2(x)=q_f e^{\delta x}$, then normalized SIFs at the both edges are equal, i.e., $K_I(-a)/\left(q\sqrt{\pi a}\right)=K_I(a)/\left(q\sqrt{\pi a}\right)$ and $K_I(-b)/\left(q\sqrt{\pi b}\right)=K_I(b)/\left(q\sqrt{\pi b}\right)$.

Finally, from tables and figures, it can be concluded that under uniform crack surface pressure, when relative thickness of the strip increases SIFs increase, too. It causes to decrease of strip's resistance. If the crack sides are loaded by fixed-grip loading, for $\delta h<0$, while thickness of the strip decreases, the normalized SIFs on axis $-Ox$ increase; but rather, the normalized SIFs on axis Ox decrease. Another point, for $\delta h>0$, while the thickness of the strip decreases, the normalized SIFs on axis $-Ox$ decrease, conversely, the normalized SIFs on axis Ox increase. Also, the cracks in the strip composed of Material 3 starts to spread faster by comparision with the strips made from Material 1 and Material 2. So, between the strips which have same geometry and same cracks, the resistance of strip made from Material 3 is the lowest. Additionally, when material orthotrophy parameter E_1/E_2 increases, SIFs increase, too. As a result, when material anisotrophy increases, critical load decreases and so strip resistance decreases.

REFERENCES

[1] Shen D, Fan TY. Exact solutions of two semi-infinite collinear cracks in a strip, Engineering Fracture Mechanics 2003; 70: 813–822.

[2] Li LH, Fan TY. Exact solutions of two semi-infinite collinear cracks in a strip of one dimensional hexagonal quasicrystal, Applied Mathematics and Computation 2008; 196: 1–5.

[3] Srisvastava KN, Palaiya RM, Karaulia DS. Interaction of shear waves with two coplanar Griffith cracks situated in an infinitely long elastic strip, Int. Journ. of Fracture; 1983; 23: 3-14.

[4] Zhou ZG, Bai YY, Zhang XW. Two collinear Griffith cracks subjected to uniform tension in infinitely long strip, International Journal of Solids and Structures 1999; 36: 5597–5609.

[5] Li XF. Closed-form solution for two collinear mode-III cracks in an orthotropic elastic strip of finite width, Mechanics Research Communications 2003; 30: 365–370.

[6] Delale F, Erdogan F. The Problem of Internal and Edge Cracks in an Orthotropic Strip, J. Appl. Mech 44(2), 237-242.

[7] Dhaliwal RS, Singh BM. Two coplanar Griffith cracks in an infinitely long elastic strip, Journal of Elasticity 1981; 11: 229-238.

[8] Dhaliwal RS, Singh BM. Two coplanar Griffith cracks in an infinite elastic layer under torsion, Journal of Engineering Mathematics 1977; 11: 337-347.

[9] Erbaş B, Yusufoğlu E, Kaplunov J. A plane contact problem for an elastic orthotropic strip. J. Engrg. Math. 2011; 70: 399-409.

[10] Erdogan F, Gupta GD, Cook TS. Numerical solution of singular integral equations. In: Sih GC, editor. Method of analysis and solution of crack problems. Leyden: Noordhoff International Publishing, 1973.

[11] Yusufoglu E, Turhan İ. A mixed boundary value problem in orthotropic strip containing a crack, Journal of the Franklin Institute 2012; 349: 2750–2769.

[12] Yusufoglu E, Turhan İ. A numerical approach for a crack problem by Gauss–Chebyshev quadrature, Arch Appl Mech 2013; 83: 1535–1547.

[13] Aleksandrov VM. Two problems with mixed boundary conditions for an elastic orthotropic strip. J. Appl. Math. Mech. 2006; 70: 128-138.

[14] Aleksandrov VM, Smetanin BI, Sobol BV. Thin Stress Concentrators in Elastic Solids, Nauka, Moskow, 1993.

[15] Aleksandrov VM, Kovalenko YeV. Problems of Continuum Mechanics with Mixed Boundary Conditions. Moscow: Nauka,1986.

[16] Lifanov IK, Saakian AV. Method of numerical solution of the problem of impressing a moving stamp into an elastic half-plane, taking heat generation into account 1982; 46: 388-394.

[17] Muskheleshvili NI. Singular Integral Equations, Edited by J.R.M. Rodok, Noordhoff International publishing Leyden, 1997.

[18] Yokus A, Baskonus HM, Sulaiman TA, Bulut H. Numerical simulation and solutions of the two-component second order KdV evolutionary system, Numerical Methods for Partial Differential Equations, 2017; 00: 1–17. https://doi.org/10.1002/num.22192, 2017.

[19] Bulut H, Tuluce Demiray S, Kayhan M. The Approximate Solutions of Time-Fractional Diffusion Equation By Using Crank Nicholson Method, Acta Universitatis Apulensis, 2014; 40: 103-112.

[20] Mason JC, Handscomb DC. Chebyshev Polynomials, CRC Press LLC, 2003.

[21] Guo LC, Wu LZ, Zeng T, Ma L. Mode I crack problem for a functionally graded orthotropic strip. European Journal of Mechanics A/Solids 2004; 23: 219–234.